

Large cone angle magnetization precession of an individual nanopatterned ferromagnet with dc electrical detection

M. V. Costache,^{a)} S. M. Watts, M. Sladkov, C. H. van der Wal, and B. J. van Wees
*Physics of Nanodevices, Materials Science Center, University of Groningen, Nijenborgh 4,
 9747 AG Groningen, the Netherlands*

(Received 5 September 2006; accepted 24 October 2006; published online 8 December 2006)

The on-chip resonant driving of large cone-angle magnetization precession of an individual nanoscale Permalloy element is demonstrated. Strong driving is realized by locating the element in close proximity to the shorted end of a coplanar strip waveguide, which generates a microwave magnetic field. A frequency modulation method is used to accurately measure resonant changes of the dc anisotropic magnetoresistance. Precession cone angles up to 9° are determined with better than 1° of resolution. The resonance peak shape is well described by the Landau-Lifshitz-Gilbert equation. © 2006 American Institute of Physics. [DOI: 10.1063/1.2400058]

The microwave-frequency magnetization dynamics of nanoscale ferromagnetic elements is of critical importance to applications in spintronics. Precessional switching using ferromagnetic resonance (FMR) of magnetic memory elements,¹ and the interaction between spin currents and magnetization dynamics are examples.² For device applications, methods are needed to reliably drive large angle magnetization precession and to electrically probe the precession angle in a straightforward way.

We present here strong on-chip resonant driving of the uniform magnetization precession mode of an individual nanoscale Permalloy (Py) strip. The precession cone angle is extracted via dc measurement of the anisotropic magnetoresistance (AMR), with angular resolution as precise as 1° . An important conclusion from these results is that large precession cone angles (up to 9° in this study³) can be achieved and detected. Moreover, measurements with an offset angle between the dc current and the equilibrium direction of the magnetization show dc voltage signals even in the absence of applied dc current, due to the rectification between induced ac currents in the strip and the time-dependent AMR.

Recently we have demonstrated the detection of FMR in an individual, nanoscale Py strip, located in close proximity to the shorted end of a coplanar strip waveguide (CSW), by measuring the induced microwave voltage across the strip in response to microwave power applied to the CSW.⁴ However, detailed knowledge of the inductive coupling between the strip and the CSW is required for a full analysis of the FMR peak shape, and the precession cone angle could not be quantified. In other recent experiments, dc voltages have been measured in nanoscale, multilayer pillar structures that are related to the resonant precessional motion of one of the magnetic layers in the pillar.^{5,6} In one case the dc voltage is generated by rectification between the microwave current applied through the structure and its time-dependent giant magnetoresistance effect.⁶ Similar voltages have been observed for a long Py strip that intersects the shorted end of a CSW, which was related in part to rectification between microwave currents flowing into the Py strip and the time-dependent AMR.⁷

Figure 1(a) shows the schematic diagram of the device used in the present work. A Py strip is located adjacent to the shorted end of a CSW and contacted with four in-line Pt leads. The CSW, Py strip, and Pt leads were fabricated on a Si/SiO₂ substrate in separate steps by conventional e-beam lithography, e-beam deposition, and lift-off techniques. The CSW consisted of 150 nm Au on 5 nm Ti adhesion layer. Figure 1(b) shows a scanning electron microscopy image of the 35 nm thick Py (Ni₈₀Fe₂₀) strip, with dimensions $3 \times 0.3 \mu\text{m}^2$ and the 50 nm thick Pt contacts (the Py surface was cleaned by Ar ion milling prior to Pt deposition to insure good metallic contacts). Pt was chosen so as to avoid picking up voltages due to the spin pumping effect.^{8,9} An AMR response of $\sim 1.7\%$ was determined for the strip by four-probe measurement of the difference ΔR between the resistances when an external magnetic field is applied parallel to the current and when it is applied perpendicular. This calibration of the AMR response will allow accurate determination of the precessional cone angle, as described below.

Microwave power of 9 dBm was applied from a generator and coupled to the CSW (designed to have a nominal 50Ω impedance) via electrical contact with a microwave probe. This drives a microwave frequency current of the order of 10 mA through the CSW, achieving the highest current density in the terminating short and thereby generating a microwave magnetic field h_1 of the order of 1 mT normal to the surface at the location of the strip. A dc magnetic field h_0 is applied along the axis of the strip, perpendicular to h_1 . In

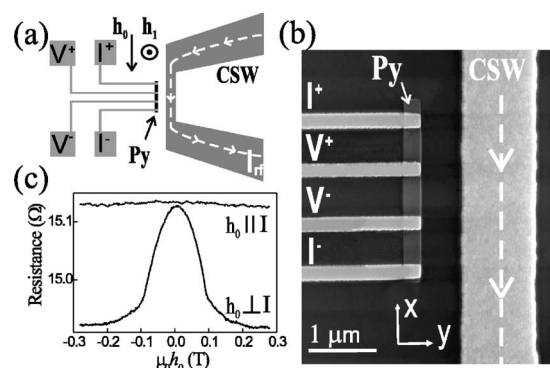


FIG. 1. (a) Schematic diagram of the device. (b) Scanning electron microscope image of device with four contacts. (c) The AMR of a typical device.

^{a)}Electronic mail: m.v.costache@rug.nl

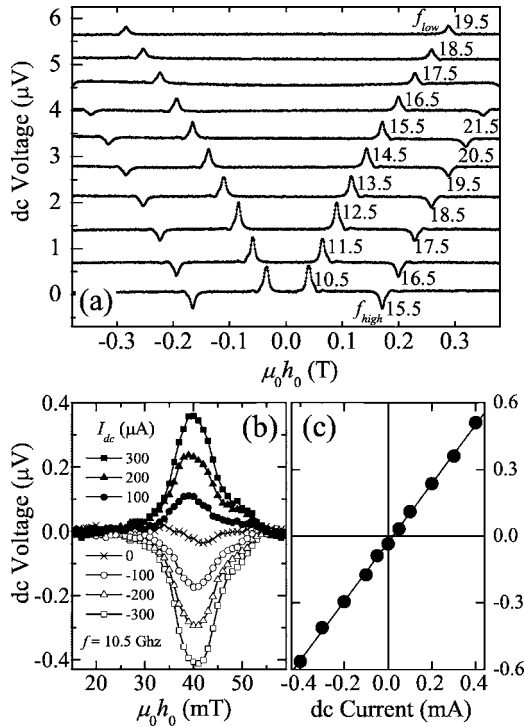


FIG. 2. (a) dc voltage measured at $I_{dc}=400 \mu\text{A}$ as a function of h_0 using the frequency modulation technique, where each curve represents $V=V(f_{\text{high}})-V(f_{\text{low}})$, with $f_{\text{low,high}}$ increasing in 1 GHz increments, and $f_{\text{high}}-f_{\text{low}}$ always 5 GHz. The curves are offset by 700 nV for clarity. (b) The peak at $f_{\text{low}}=10.5$ GHz for a number of currents between -300 and $300 \mu\text{A}$. (c) The peak height from the data in (b) plotted vs the current. The line is a linear fit to the data.

this geometry we have previously shown that we can drive the uniform FMR precessional mode of the Py strip.⁴ All measurements were performed at room temperature.

In the AMR effect [see Fig. 1(c)], the resistance depends on the angle θ between the current and the direction of the magnetization as $R(\theta)=R_0-\Delta R \sin^2 \theta$, where R_0 is the resistance of the strip at $h_0=0$. When the dc current and the equilibrium magnetization direction are parallel and the magnetization of the Py undergoes circular, resonant precession about the equilibrium direction, the dc resistance will decrease by $\Delta R \sin^2 \theta_c$, where θ_c is the cone angle of the precession. Since the shape anisotropy of our Py strip causes deviation from circular precession, θ_c is an average angle of precession.

We have used a frequency modulation method in order to better isolate signals due to the resonance state, removing the background resistance signal due to R_0 and dc voltage offsets in the amplifier. In this method, the frequency of the microwave field is alternated between two different values 5 GHz apart, while a dc current is applied through the outer contacts to the strip. A lock-in amplifier is referenced to the frequency of this alternation (at 17 Hz), and thus measures the difference in dc voltage across the inner contacts between the two frequencies, $V=V(f_{\text{high}})-V(f_{\text{low}})$. Only the additional voltage given by the FMR-enhanced AMR effect will be measured when one of the microwave frequencies is in resonance.

Figure 2(a) shows a series of voltage vs field curves in which both f_{low} and f_{high} are incremented in 1 GHz intervals at a dc current of $400 \mu\text{A}$. The curves feature dips and peaks at magnetic field magnitudes corresponding to the magnetic

resonant condition with either f_{high} or f_{low} , respectively. In Fig. 2(b) we focus on the peak for $f=10.5$ GHz, and show curves for different currents ranging from -300 to $+300 \mu\text{A}$. The peak height scales linearly with the current as expected for a resistive effect [Fig. 2(c)]. From the slope of $1.325 \text{ m}\Omega$ we obtain an average cone angle $\theta_c=4.35^\circ$ for this frequency.³ Interestingly, in Fig. 2(b) a small, somewhat off-center dip is observed even for zero applied current, giving an intercept of -30 nV in Fig. 2(c). We will discuss this in detail later in this letter.

To extract information about the magnetization dynamics from the peak shape, we use the Landau-Lifshitz-Gilbert (LLG) equation, $d\mathbf{m}/dt=-\gamma\mathbf{m}\times\mu_0\mathbf{H}+(\alpha/m_s)\mathbf{m}\times d\mathbf{m}/dt$, where $\mathbf{H}=(h_0-N_xm_x,-N_y m_y,h_1-N_z m_z)$ includes the demagnetization factors N_x , N_y , and N_z (where $N_x+N_y+N_z=1$), $\gamma=2/\pi 28 \text{ GHz/T}$ is the gyromagnetic ratio, α is the dimensionless Gilbert damping parameter, and m_s is the saturation magnetization of the strip. Due to the large aspect ratio of the strip, N_x can be neglected. In the small angle limit ($dm_x/dt=0$, such that $m_x\approx m_s$) the LLG equation can be linearized. In response to a driving field $h_1 \cos \omega t$ with angular frequency ω , we express the solutions as a sum of in-phase and out-of-phase susceptibility components, so $m_y=\chi'_y(\omega)h_1 \cos \omega t+\chi''_y(\omega)h_1 \sin \omega t$ and $m_z=\chi'_z(\omega)h_1 \cos \omega t+\chi''_z(\omega)h_1 \sin \omega t$. The components for m_y are as follows:

$$\chi'_y(\omega)=-\frac{m_s}{2h_c+m_s(\gamma\mu_0/\omega)^2(h_0-h_c)^2+\alpha^2},$$

$$\chi''_y(\omega)=\frac{m_s}{2h_c+m_s(\gamma\mu_0/\omega)^2(h_0-h_c)^2+\alpha^2}(\gamma\mu_0/\omega)(h_0-h_c). \quad (1)$$

The components of m_z are related to those of m_y by $\chi'_z=\alpha\chi'_y-(\gamma\mu_0/\omega)(h_c+N_y m_s)\chi''_y$ and $\chi''_z=\alpha\chi''_y+(\gamma\mu_0/\omega h_1)(h_c+N_y m_s)\chi'_y$. The resonance field h_c for the uniform precessional mode is related to ω by Kittel's equation,

$$\omega^2=\gamma^2\mu_0^2(h_c+(1-N_y)m_s)(h_c+N_y m_s). \quad (2)$$

The precession angle $\theta_c(t)$ is determined from the relation $\sin^2 \theta_c(t)=\theta_c^2(t)=(1/m_s^2)(m_y^2+m_z^2)$. We find that θ_c^2 can be written as the sum of a time-independent term and terms with time dependence at twice the driving frequency, $\theta_c^2=\theta_{\text{dc}}^2+\theta_c^2(2\omega)$, where $\theta_{\text{dc}}^2=(1/2)(h_1/m_s)^2(\chi_y'^2+\chi_y''^2+\chi_z'^2+\chi_z''^2)$. The dc voltage is calculated to be

$$V=A\frac{1}{(\gamma\mu_0/\omega)^2(h_0-h_c)^2+\alpha^2}, \quad (3)$$

where $A=(1/2)I_{\text{dc}}\Delta R(h_1/2h_c+m_s)^2(1+(\gamma\mu_0/\omega)^2(h_c+N_y m_s)^2)$. Each peak from the data shown in Fig. 2(b) has been averaged with peaks at the same frequency, and replotted in Fig. 3(a) as a function of $\gamma\mu_0 h_0/\omega$. The solid lines are fits of Eq. (3) to the data, in which A and h_c are free fit parameters for each curve, and we have required α to be the same for all of the peaks, resulting in a best-fit value $\alpha=0.0104$. A plot of the frequency versus the center position of each peak h_c is shown in Fig. 3(b). The excellent fit of Eq. (2) to the data verifies that this is the uniform precessional mode, and yields values of $\mu_0 m_s=1.06 \text{ T}$ and $N_y=0.097$ as fit parameters. With these values we can extract the driving field h_1 from the peak fit parameter A [Fig. 3(c)]. In agreement with our initial estimates, the field is of the order of 1 mT, but drops off by roughly a factor of 2 between 10 and

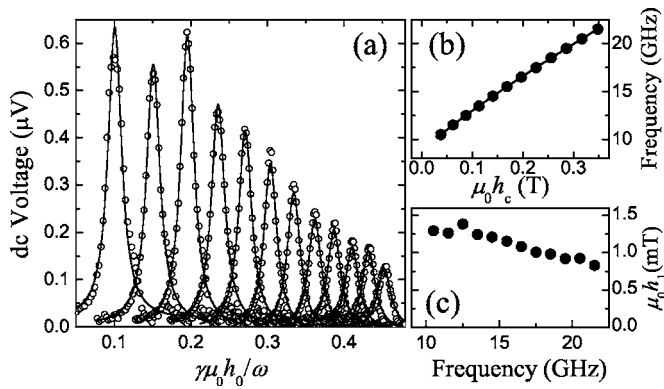


FIG. 3. (a) Resonant peaks at various frequencies ranging from 10.5 to 21.5 GHz in 1 GHz steps as a function of the field h_0 normalized to the frequency. Solid lines are the fits of Eq. (3) to the data. (b) The frequency of the peak vs its center position h_c . The line is a fit of Eq. (2) to the data. (c) The field h_1 calculated from the fit coefficients to the data in (a) and (b) as a function of frequency.

20 GHz, consistent with frequency dependent attenuation of our microwave cables and probes.

We now discuss the observation of dc voltages in the absence of any applied dc current. In our device, there are microwave currents induced in the strip and detection circuit due to capacitive and inductive couplings to the CSW structure, and thus there is the possibility for rectification between the time-dependent AMR and induced microwave currents. We express the induced current as a sum of in-phase and out-of-phase components, $I_{in} = I_1 \cos \omega t + I_2 \sin \omega t$.

For rectification to occur, the resistance must also have first harmonic components. As mentioned earlier, the elliptical precession of the magnetization gives a time dependent term for the cone angle $\theta_c^2(2\omega t)$, but this is only at the second harmonic and cannot produce rectification. However, if there is an offset angle ϕ between the applied field and the long axis of the strip, then the AMR term is approximately $-\Delta R(\sin^2 \phi + (m_y(t)/m_s)\sin 2\phi)$, obtained by taking a small angle expansion of $\theta_y(t) = m_y(t)/m_s$ about ϕ . Multiplying with the current yields a dc voltage term

$$V = -\frac{1}{2} \frac{h_1}{m_s} \Delta R (I_1 \chi'_y + I_2 \chi''_y) \sin 2\phi. \quad (4)$$

Figure 4 shows resonance peaks at $f=17.5$ GHz and at $f=12.5$ GHz for five different angles between the applied field and the long axis of the strip. The zero angle ($\phi=0$) is with respect to the geometry of our setup; however, it is possible that there is some offset angle ϕ_0 at this position. For the 17.5 GHz data, rotating the field by -5° causes the peak to practically disappear. At -10° the peak reverses sign. This is in agreement with Eq. (4), with an offset angle $\phi_0 = -5^\circ$. However, the data at $f=12.5$ GHz show almost no peak signal already at $\phi=0$ even though there has been no change in the setup. Moreover, in this data we more clearly see contribution from a dispersive line shape, corresponding to the $I_2 \chi''_y$ term in Eq. (4). For each frequency, we fit Eq. (4) to all the curves simultaneously, where we have used the parameters for the magnetization extracted earlier and allowed only I_1 , I_2 , and an offset angle ϕ_0 to be free parameters. For the 17.5 GHz data, we obtain $\phi_0 = -6.1^\circ$, $I_1 = -28 \mu A$, and $I_2 = 8 \mu A$. For the 12.5 GHz data, we obtain $\phi_0 = -1.5^\circ$, I_1

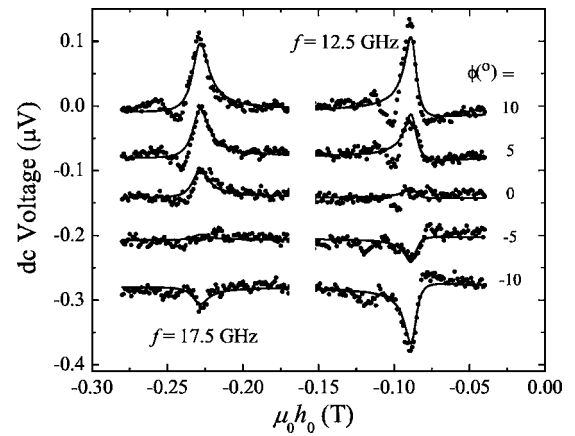


FIG. 4. Voltage peaks at $f=17.5$ GHz (left) and at $f=12.5$ GHz (right) without any applied dc current for different angles ϕ between the h_0 and the long axis of the strip. Solid lines are fits of Eq. (4) to the data.

$= 23 \mu A$, and $I_2 = 11 \mu A$. The large difference in ϕ_0 between 12.5 and 17.5 GHz is likely due to a frequency dependence of the induced currents and how they flow through the Pt contacts to the Py.

The method and analysis presented here are valid for any ferromagnet under the conditions that it exhibits AMR and a uniform FMR precession mode. Additional anisotropy fields in hard ferromagnets will modify the Kittel equation [Eq. (2)]. Situations in which a uniform precession mode cannot be obtained, such as when there are multiple domains and/or resonant modes,¹⁰ could also be detected by AMR but will require a more sophisticated analysis. For the purposes of this experiment we have used a relatively long strip geometry with four in-line contacts. However, two contacts are sufficient and there is no particular limit to how small the ferromagnetic element can be, as long as it can be electrically contacted and dc current applied along the equilibrium magnetization direction. In terms of resolution, we estimate that precessional cone angles as precise as 1° can be resolved.

This work was financially supported by the Dutch Organization for Fundamental Research on Matter (FOM). The authors acknowledge J. Jungmann for her assistance in this project.

¹S. Kaka and S. E. Russek, Appl. Phys. Lett. **80**, 2958 (2002).

²M. Tsoi, A. G. M. Jansen, J. Bass, W.-C. Chiang, V. Tsoi, and P. Wyder, Nature (London) **406**, 46 (2000).

³At 13 dBm of applied power, we have measured an angle of $\theta_c = 9.0^\circ$ at $f=10.5$ GHz. We focus here on the 9 dBm data, however, since we can apply this power over the entire 10 to 25 GHz bandwidth.

⁴M. V. Costache, M. Sladkov, C. H. van der Wal, and B. J. van Wees, Appl. Phys. Lett. **89**, 192506 (2006).

⁵A. A. Tulapurkar, Y. Suzuki, A. Fukushima, H. Kubota, H. Maehara, K. Tsunekawa, D. D. Djayaprawira, N. Watanabe, and S. Yuasa, Nature (London) **438**, 339 (2005).

⁶J. C. Sankey, P. M. Braganca, A. G. F. Garcia, I. N. Krivorotov, R. A. Buhrman, and D. C. Ralph, Phys. Rev. Lett. **96**, 227601 (2006).

⁷A. Yamaguchi, T. Ono, Y. Suzuki, S. Yuasa, A. Tulapurkar, and Y. Nakatani, e-print cond-mat/0606305.

⁸A. Brataas, Y. Tserkovnyak, G. E. W. Bauer, and B. I. Halperin, Phys. Rev. B **66**, 060404(R) (2002).

⁹M. V. Costache, M. Sladkov, S. M. Watts, C. H. van der Wal, and B. J. van Wees, Phys. Rev. Lett. **97**, 216603 (2006).

¹⁰J. Grollier, M. V. Costache, C. H. van der Wal, and B. J. van Wees, J. Appl. Phys. **100**, 024316 (2006).